New observations of recently active wrinkle ridges in the lunar mare: Implications for the timing and origin of lunar tectonics

Cole A Nypaver[1] and Bradley J Thomson[1]

[1]University of Tennessee

November 22, 2022

Abstract

The variety of tectonic features on the Moon indicates that the lunar lithosphere has undergone a complex deformational history. Lobate scarps and wrinkle ridges are two such tectonic features that have resulted from compressional stresses. The crisp morphologies and cross cutting relations associated with a global population of lobate scarps have been cited as evidence for their recent (<50 Ma) formation, but observations of recently active wrinkle ridges have yet to be made on a similar scale. Here, we present new observations of 1,127 recently active wrinkle ridge segments on the lunar nearside mare. Our results indicate that recently active wrinkle ridges are distributed across ~90% of nearside mare basins – occurring in clusters of ~10–100 ridge segments with a mean segment length of 4.4 km. The magnitudes and orientations of these recently active wrinkle ridges are consistent with the hypothesis of formation by orbital recession stresses.

New observations of recently active wrinkle ridges in the lunar mare: Implications for the timing and origin of lunar tectonics

C. A. Nypaver[1], B. J. Thomson[1]

[1] Department of Earth and Planetary Sciences, University of Tennessee Knoxville, Knoxville, TN, 37966

Corresponding author: Cole Nypaver (cnypaver@vols.utk.edu)

Key points:

- Young (<50 Ma) wrinkle ridges are widespread across the lunar nearside lunar mare as a result of recent tectonic activity.

- The most recently active wrinkle ridges on the lunar mare occur in clustered networks and exhibit narrow, sinuous morphologies.

- The scale and preferred orientations of the recently active wrinkle ridges presented here suggest formation by tidal and impact stresses.

Abstract

The variety of tectonic features on the Moon indicates that the lunar lithosphere has undergone a complex deformational history. Lobate scarps and wrinkle ridges are two such tectonic features that have resulted from compressional stresses. The crisp morphologies and cross cutting relations associated with a global population of lobate scarps have been cited as evidence for their recent (<50 Ma) formation, but observations of recently active wrinkle ridges have yet to be made on a similar scale. Here, we present new observations of 1,127 recently active wrinkle ridge segments on the lunar nearside mare. Our results indicate that recently active wrinkle ridges are distributed across ~90% of nearside mare basins – occurring in clusters of ~10–100 ridge segments with a mean segment length of 4.4 km. The magnitudes and orientations of these recently active wrinkle ridges are consistent with the hypothesis of formation by orbital recession stresses.

Plain Language Summary

The surface of Earth's Moon has undergone continual shifting for ~4 billion years in response to a variety of compressional forces. Recent studies of small, linear faults in the lunar surface, known as lobate scarps, have indicated that those features formed within the last ~50 million years and may remain currently active. A separate class of compressional features, known as wrinkle ridges, exist primarily in the solidified lava flows on the lunar nearside. The timing and formative mechanisms associated with those recently formed wrinkle ridges remain under constrained. Here, we present new observations and measurements of a large population of small wrinkle ridges on the lunar nearside. Many of the features that we document in this work have yet to be studied in detail, and our results indicate that the forces associated with the migration of the Moon away from Earth are responsible for their formation.

1 Introduction

The surface of the Moon boasts an array of tectonic features. Compressional stresses acting on the lunar lithosphere have manifested in the form of lobate scarps and wrinkle ridges across the lunar highlands and mare (e.g., Schultz, 1976). Evidence for the recent movement and formation of lunar lobate scarps has been put forth in the form of cross cutting relations with other, young lunar surface features (e.g., Binder, 1982; Watters et al., 2012) as well as absolute model ages derived from buffered crater counting over those scarps (Clark et al., 2017; Van der Bogert et al., 2018). The spatial distribution and orientations of lunar lobate scarps have indicated that some combination of orbital recession, global contraction, and solid-body tidal stresses are at work in deforming the lunar lithosphere on a global scale (e.g., Watters et al., 2010; Banks et al., 2012; Watters et al., 2015). The extensive knowledge base regarding recent lunar tectonism is derived primarily from these robust studies of lobate scarps.

Compared to the near-global distribution of lobate scarps, wrinkle ridges on the lunar surface exist primarily in the lunar maria (Schultz, 1976; Melosh, 1978; Watters et al., 2022). Early wrinkle ridge formation in the lunar maria resulted from an isostatic response of the lunar lithosphere to the voluminous outpouring of mare deposits onto the lunar surface (e.g., Melosh, 1978). The formation of those early wrinkle ridges followed a predictable geometric pattern in which linear wrinkle ridges formed in radial and concentric patterns away from the mascon center (e.g., Melosh, 1978; Solomon and Head, 1980; Freed et al., 2001). Morphologically, most wrinkle ridges exhibit increased lengths, widths, and topographic relief relative to lunar lobate scarps.

The regional distribution and ages of those larger, mascon-induced wrinkle ridges have been analyzed using Lunar Reconnaissance Orbiter Camera (LROC) Wide Angle Camera (WAC) data with an image resolution of 100 m/px (Yue et al., 2019; Schleicher et al., 2019; Li et al., 2018). Recent work has also successfully utilized rock abundance data derived from LRO Diviner instrument thermal data to identify a network of recently active wrinkle ridges on the lunar nearside (Bandfield et al., 2011; Valantinas and Schultz, 2020). However, the resolution of the rock abundance dataset is coarser (237 m/px) than that of the LROC WAC image data. The use of those coarse resolution data in prior work prohibited the observation of any smaller, decameter-wide wrinkle ridges that may be below the resolution of the LROC WAC dataset. The omission of small, recently active wrinkle ridges from past work has the potential to introduce a sampling bias into the understanding and timing of wrinkle ridge formation and global stress mechanisms acting on the lunar lithosphere.

Several recent studies have identified subsets of recently active wrinkle ridges that do not follow the paradigm of mascon tectonism (e.g., Williams et al., 2019; Lu et al., 2019; Clark et al., 2022). These recently active ridges, located in isolated regions of Mare Frigoris, Mare Serenitatus, and Mare Imbrium, crosscut meter scale impact craters and display crisp, uneroded morphologies – potentially indicating recent formation by localized, late-stage mare cooling (Lu et al., 2019) or lunar global contraction (Williams et al., 2019). However, those studies present isolated results over only a small percentage of the nearside mare.

Until now, interpretations regarding global stress mechanisms currently acting on the lunar lithosphere have been primarily derived from observations and measurements of lobate scarps in the lunar highlands and large-scale wrinkle ridges in the nearside lunar mare. Here, we present new observations of small, recently active wrinkle ridges across ~90% of the lunar nearside mare. Our work therefore stands to provide a more spatially complete understanding of stress mechanisms that are responsible for recent deformation of the lunar surface and lithosphere. Given that our results are constrained to the mare, this work also provides new regions of interest for a future lunar geophysical network that are advantageous to a wider variety of geologic subdisciplines.

2 Methods

We utilized NAC images from the LROC instrument in the LROC Quickmap web interface to identify tectonically deformed impact craters across the lunar maria with diameters ranging from <30 m to >2 km. The specific NAC image data used in our work consisted of an LROC Wide Angle Camera (WAC; 100 m/px) mosaic overlaid with large incidence (55–80˚) NAC images (0.5–2.0 m/px) and NAC region of interest (ROI) mosaics (0.5–2.0 m/px) where available (WAC+NAC+NAC_ROI_MOSAIC toggle in the Quickmap layers menu). As the NAC mosaics are only available for specific, larger surface features, the overwhelming majority of our mapping was conducted using the individual NAC image swaths. A shapefile of 11,746 previously mapped wrinkle ridges was overlain onto these image data to provide a general sense of wrinkle ridge location throughout the lunar maria (Thompson et al., 2017). The individual wrinkle ridges mapped in that work exhibit a mean length of 15.8 km and a total, combined length of 94,824 km. Those previously identified ridges were mapped in LROC WAC image data at a larger scale than that used in our methods. We manually examined each wrinkle ridge under or near to those polyline features in the Thompson et al., 2017 dataset and placed a point feature at the center of every identifiable impact crater that had been deformed in some way by a wrinkle ridge.

Two geologic scenarios justified the classification of an impact crater as tectonically deformed in our mapping (**Fig. 1**): (1) the impact crater was directly crosscut by both bounding scarps of a wrinkle ridge, or (2) if a crater has been infilled or crosscut by one of two bounding scarps associated with the crosscutting ridge. While the former scenario comprised the majority of crater deformation in our dataset, a small percentage of the latter were observed as well. Once the deformed craters were flagged as tectonically deformed in Quickmap, the database of deformed crater center points was exported into ESRI's ArcGIS Pro as a point shapefile. That point shapefile was then used to create a density map of deformed crater populations using the ArcGIS Kernel Density tool.

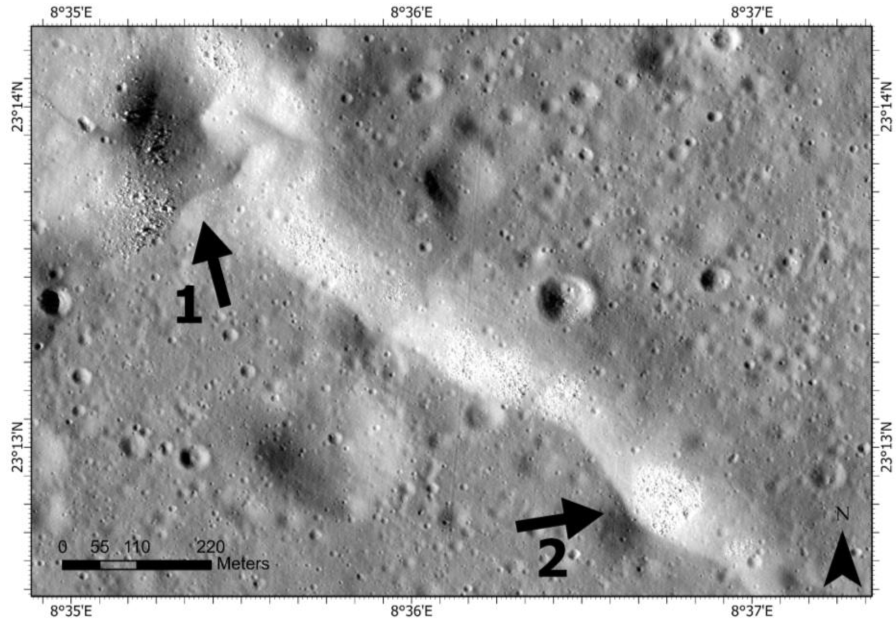

Figure 1: LROC NAC image showing the two primary types of cross cutting relationships used to map tectonically deformed impact craters in our work: 1) a degraded crater crosscut by both parallel wrinkle ridge scarps and 2) crater deformation by a single wrinkle ridge scarp (LROC NAC M1354091640LE).

We used our point density map of tectonically deformed impact craters to identify isolated areas of increased tectonic activity across the lunar nearside mare. Each zone typically contained an isolated complex of small, sinuous ridges that were responsible for the majority of crater deformation in that zone. We used the same NAC image data (0.5–2.0 m/px) in the LROC Quickmap interface to then map those individual ridge segments within the zones of recent activity. Our mapping effort was conducted at a smaller scale using higher resolution image data than was used in previous wrinkle ridge analyses (e.g., Thompson et al., 2017; Yue et al., 2019).

163 **3 Results**

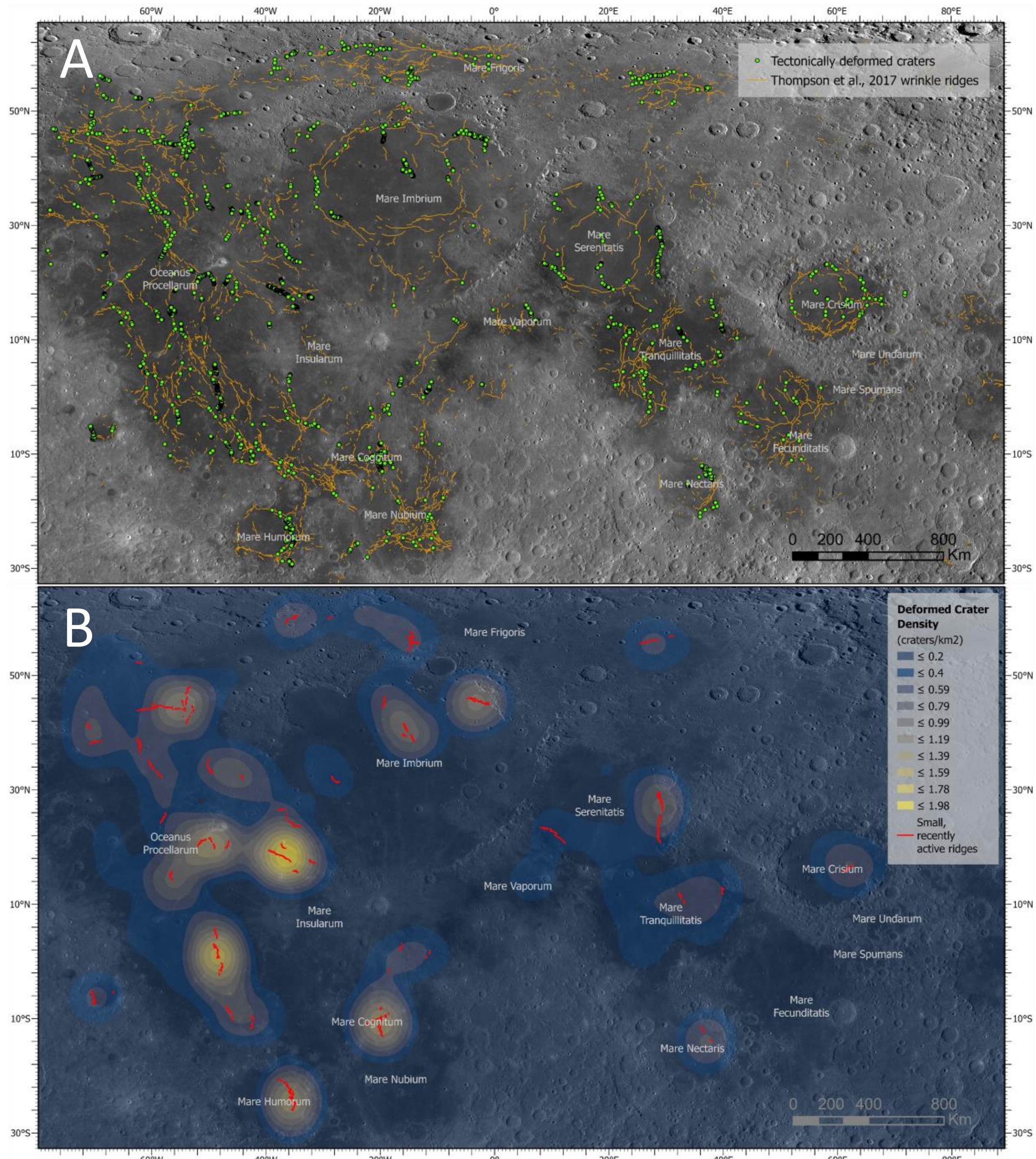

Figure 2: (A) Previously mapped wrinkle ridges (Thompson et al., 2017 - orange line features) and 2,277 tectonically deformed impact craters identified in this study (green point features) overlying an LROC WAC mosaic of the lunar nearside mare. (B) Density map of the tectonically deformed impact craters given in part (A) overlain by the recently active wrinkle ridge segments (red line features). Under the assumption that the most recently active ridges cause the most observable surface deformation, east and south Oceanus Procellarum exhibit the most recent tectonic activity on the nearside mare.

Using LROC NAC images in the LROC Quickmap interface, we mapped 2,277 impact craters in the diameter range of ~0.03–2.0 km on the nearside lunar mare that have been deformed by compressional tectonic activity (**Fig. 2A**). Most of those mapped craters were deformed by 1,152 wrinkle ridge segments distributed across 37 isolated "zones" of recent tectonic activity in the nearside lunar mare (**Fig. 2B**). The mapped wrinkle ridge segments exhibit a mean length of 4.4 km and combined length of 5,070 km. The isolated zones of recent tectonic activity can be observed as areas of dense surface deformation in our crosscut crater map (**Fig. 2B**). Morphologically, the wrinkle ridges mapped here exhibit narrow widths (~100–300 m), measurable sinuosity ratios of <1.5, and relatively minimal topographic relief. In cross section, the small ridges commonly exhibit narrow central ridges with steeply sloping bounding scarps that are superposed on more broad topographic arches (**Fig. 3**). This cross-sectional morphology is common among other lunar wrinkle ridges of varying sizes. A dendritic pattern was observed among individual ridge clusters in which narrow, sinuous ridges propagated parallel to and away from one another in a single,

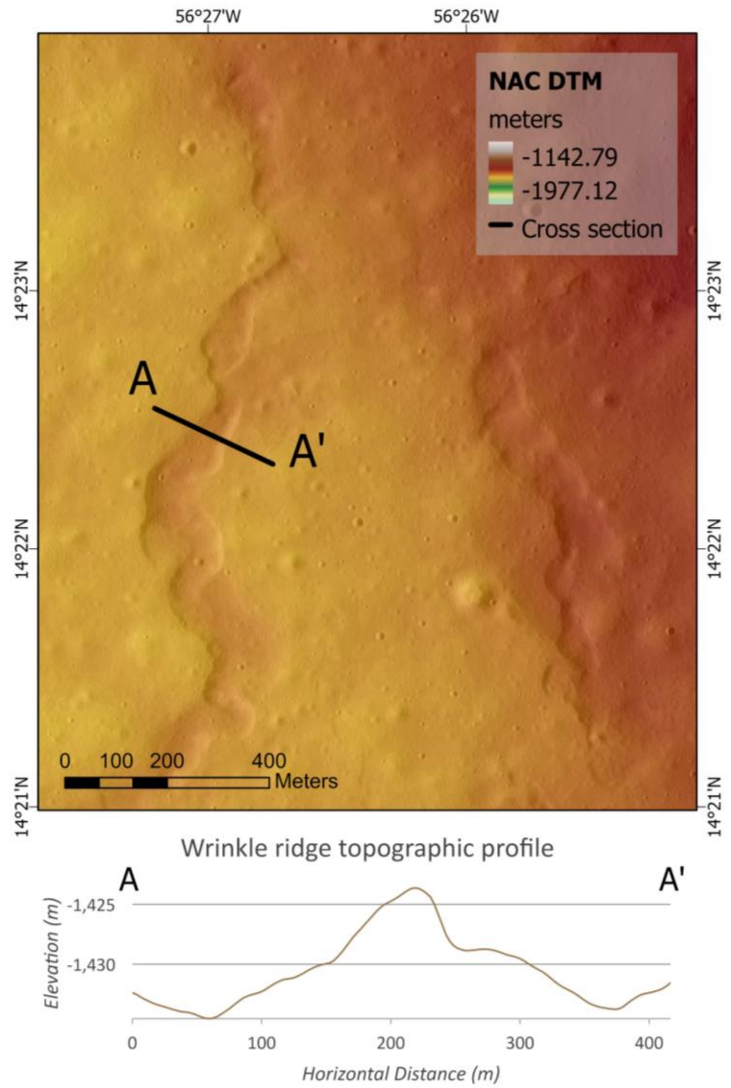

Figure 3: LROC NAC image (Marius Cone ROI mosaic) of a wrinkle ridge complex located in central Mare Procellarum overlaid by and LROC NAC Digital Terrain Model (DTM; Marius Cone 1). In cross section, the ridge system here exhibits a narrow (~100 m) central ridge with a steep southeast facing scarp that is underlain by a broader (~300 m) topographic arch. At center, the ridge exhibits ~12 m in total relief.

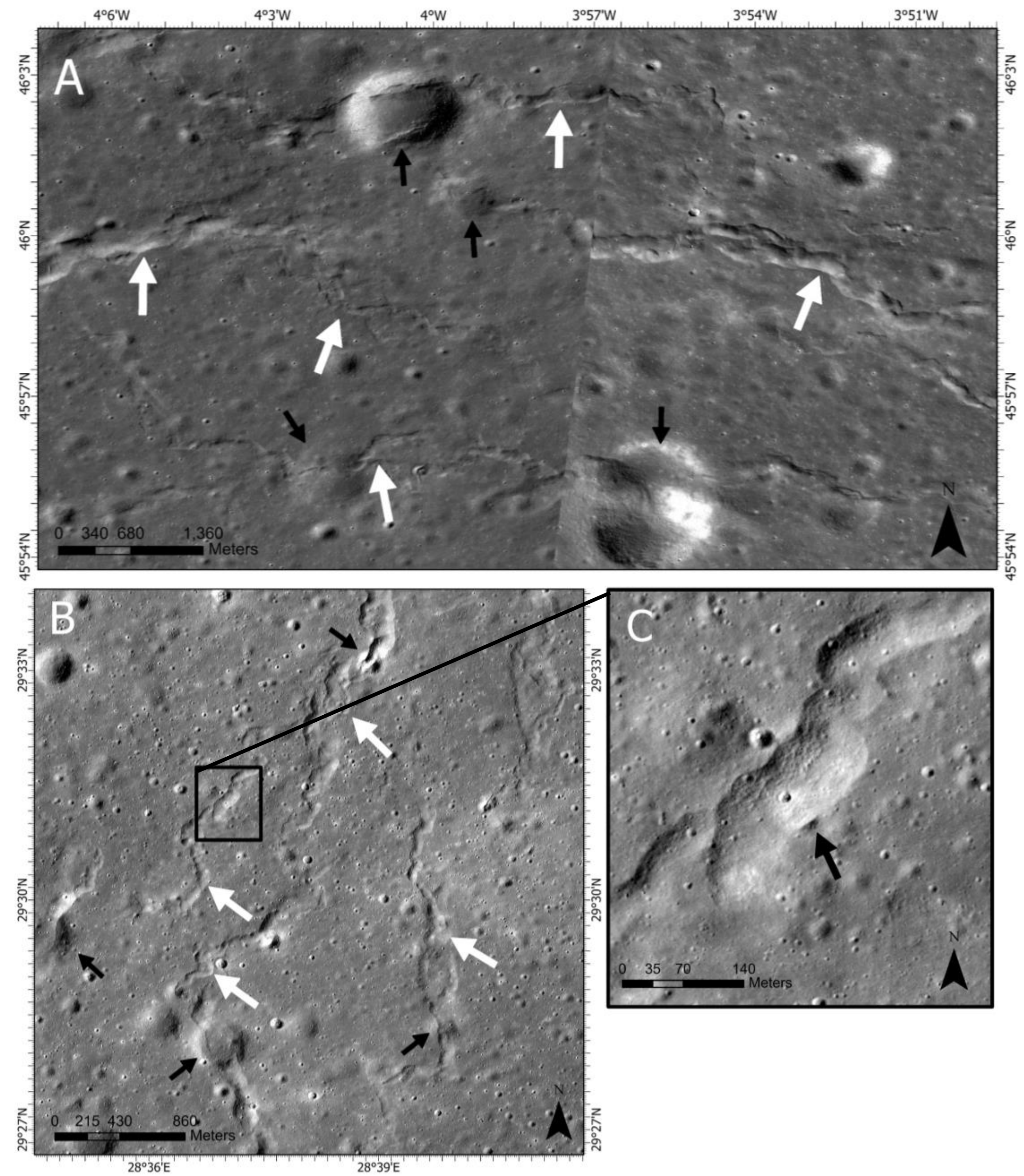

Figure 4: Recently active wrinkle ridge systems located in N. Mare Imbrium (A) (LROC NAC M1274280167RE, M1236649139LE) and E. Mare Serenitatus (B) (LROC NAC M1289319410LE). (C) Image subset depicting a ~35 m-diameter impact crater crosscut by a recently active wrinkle ridge. White arrows indicate recently active ridges and black arrows show crosscut craters in all images.

overarching direction (**Fig. 4**). Regionally, the small, sinuous ridges demonstrated a preferred NNW-SSE orientation at equatorial latitudes (30˚S–30˚N) that shallowed to a preferred WNW-ESE orientation at higher latitudes (30˚N–60˚N) (**Fig. 5**).

4 Discussion

The small wrinkle ridges identified here crosscut impact craters on the lunar surface with diameters as small as ~30 m (**Fig. 4c**). Based on current models of regolith overturn and impact crater topographic diffusion, past studies have cited similar cross cutting of meter-to-decameter scale impact craters as evidence for recent (<50 Ma) or current movement of the associated ridge (Trask, 1971; Moore et al., 1980; Fassett and Thomson, 2014; Speyerer et al., 2016; Williams et al., 2019). Our results indicate that these recently active wrinkle ridge systems exist in 37 locations across most nearside mare basins (**Fig. 2B**). Buffered crater counting methods have been used in past studies to establish absolute model ages (AMAs) for larger wrinkle ridges on the lunar surface (Yue et al., 2017), but that work was limited by the resolution of the LROC WAC data (100 m/px). The use of lower resolution data in that work resulted in the exclusion of the meter-scale wrinkle ridges and crosscut craters identified here. The derived wrinkle ridge AMAs (~3.1–3.5) were, therefore, much older than those postulated for the small, sinuous ridges identified here. Similar AMAs for the small, recently active ridges identified here are difficult to obtain due to a lack of superposing craters, non-linear ridge morphologies, and the tectonically altered diameters of the craters that have been crosscut.

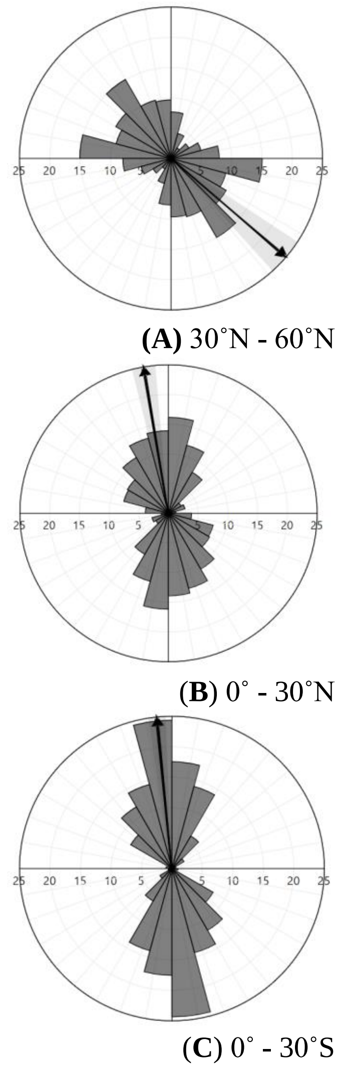

Figure 5: Rose diagrams showing the preferred orientations of recently active, small wrinkle ridges (Fig. 2A) between (A) 30˚N and 60˚N, (B) 0˚ and 30˚N, and (C) 0˚ and 30˚ S. Arrows indicate preferred orientations.

Several stress mechanisms have been proposed to account for the formation of young lunar tectonic features on the lunar surface. Large-scale, radial wrinkle ridges located in the nearside mare basins have been postulated to result from lithospheric compensation in response to mare formation and isostatic loading of the lunar lithosphere (Melosh et al., 1978; Solomon and head, 1980; Freed et al., 2001). Separately, the global distribution and preferred N-S orientation of recently active lobate scarps at equatorial latitudes has been cited as evidence for lithospheric flexure due to lunar orbital recession aided by global contraction (Melosh, 1978; Melosh, 1980; Watters et al., 2015; 2019). Operating under the assumption that the presence of dense boulder fields on a wrinkle ridge indicates recent tectonic movement of that ridge, another recent study utilized the LRO Diviner rock abundance dataset to identify a network of recently active wrinkle ridges that exhibited heightened boulder populations on their scarp slopes (Bandfield et al., 2011; Valantinas and Schultz, 2020). The recently active ridges in that work were coincident with a deep-seated rift network inferred from polygonal lineations in Gravity Recovery and Interior Laboratory (GRAIL) gravity gradient data (Andrews-Hanna et al., 2014). The observed recent tectonism was therefore attributed to a reactivation of that deep seated fault system by a stress network that is antipodal to and caused by the SPA impact event (Schultz and Crawford, 2011; Valantinas and Schultz, 2020). Lastly, two separate wrinkle ridge complexes in east Mare Serenitatus and north Mare Imbrium have been presented as being recently active due to potential late-stage mare cooling and global contraction stresses, respectively (Lu et al., 2019; Clark et al., 2022). Morphologically, the small, sinuous ridges analyzed in those studies are the most similar to those mapped in here. As such, both were included in our database of recently active ridges on the nearside mare.

Several of the aforementioned stress mechanisms can be ruled out as the cause of recent wrinkle ridge activity identified in our work. Unlike the larger, more evenly distributed wrinkle ridges associated with a mascon tectonic system, the recently active ridges presented here are narrow and sinuous in morphology and often occur in branching clusters of ~10–100 individual ridge segments in both mascon and non-mascon settings. Prior studies have also concluded that formation of mascon-related wrinkle ridge formation ceased at ~1.2 Ga based on crosscutting relationships with other surface features (Melosh et al., 1978; Solomon and Head, 1980; Freed et al., 2001). Thus, causation by mascon isostatic compensation is disfavored as a formation hypothesis due to the differential scale and timing of the ridges associated with that stress mechanism. The hypothesis of late-stage mare cooling as causation for recent tectonism is partially supported by non-KREEP-bearing lunar samples returned by the Chang'e 5 mission that exhibit radiometric age dates of ~2.0 Ga. Prolonged cooling or volcanism within the lunar mare is necessary to justify such a young crystallization age (e.g., Tian et al., 2021). However, given the time disparity between the pervasive ridge activity documented here (<50 Ma) and the expected cessation of mare volcanism (~1.0 Ga; Schultz and Spudis, 1983; Heisinger et al., 2011), we expect localized flow cooling and contraction to be an unlikely sole cause of widespread, recent tectonism in the lunar nearside mare.

The ridges mapped in our work exhibit preferred NNW-SSE linear orientations at near-equatorial latitudes (0˚–30˚ S, 0˚–30˚ N) that gradually shallow to WNW-ESE orientations at greater distances from the lunar equator (30˚N–60˚ N) (**Fig. 5**). These fault orientation patterns are consistent with those expected from lunar orbital recession stresses and relaxation of a nearside tidal bulge (e.g., Figure 2C in Watters et al., 2015). A small number of the recently active ridges mapped here also appear to be spatially correlated with GRAIL gravity gradient data. Such a correlation is consistent with causation by an antipodal SPA stress network and associated deep moonquakes centered beneath the lunar nearside mare (Valantinas and Schultz, 2020; Schultz and Crawford, 2011). One primary difference between these two potential stress mechanisms is the scale of tectonic deformation that results from each. The surface expression of an SPA antipodal stress release has been identified as a reactivation of deep-seated faults and a shifting of larger wrinkle ridges associated with those faults (Valantinas and Schultz, 2020). The lower lithospheric stresses imparted by orbital recession (~20–40 KPa) are more likely to result in smaller tectonic landforms that are limited in width, length, and depth of deformation (Watters et al., 2015). The narrow, sinuous morphologies associated with many of the ridges mapped in our work appear more consistent with formation by those lithospheric stresses imparted by orbital recession and despinning. However, given the close spatial correlation between several recently active ridges and deep-seated faults inferred from GRAIL gravity gradient data (i.e., Mare Frigoris, Mare Serenitatus, and Oceanus Procellarum), SPA antipodal stresses should not be ruled out as a formation mechanism on a local scale. The addition of a secondary, SPA-induced stress mechanism helps to explain the few local deviations from the overall NNW-SSE orientation observed in our wrinkle ridge dataset.

5 Conclusions

Through extensive mapping of recently active lunar wrinkle ridges and tectonically deformed impact craters, we have presented new observations of recent tectonic deformation on the lunar nearside mare. From those results, we put forth the following conclusions.

- We identify tectonically deformed impact craters on the lunar mare with diameters as small as ~30 m. Models of regolith overturn and crater diffusion indicate that impact craters on this diameter scale should be erased from the lunar surface in <50 Ma (Trask, 1971; Moore et al., 1980; Fassett and Thomson, 2014; Speyerer et al., 2016; Williams et al., 2019). Thus, the superposing wrinkle ridges mapped here have been geologically active in at least an equivalent timeframe.

- Individual ridges identified in our work display narrow, sinuous morphologies and are spatially clustered in 37 isolated areas across most nearside mare basins. These recently active ridge clusters occur at the centers and edges of both mascon and non-mascon mare, indicating that their formation and activity is likely unrelated to mare thickness or isostatic compensation of the lunar lithosphere.

- The recently active wrinkle ridge segments documented here exhibit a preferred NNW-SSE orientation at equatorial latitudes that that shallow to a WNW-ESE orientation with increased latitude. When combined with the small morphological scale of the recently active ridges presented here, this latitude-dependent orientation pattern is consistent with formation by orbital recession stresses and tidal bulge relaxation – a mechanism that has been hypothesized as the cause of recently active lobate scarps in the lunar highlands (e.g., Watters et al., 2015). However, given the spatial coincidence between several recently active ridges and deep-seated faults inferred from GRAIL gravity gradient data, SPA antipodal stresses should not be ruled out as formative stress on a local scale (e.g., Valantinas and Schultz, 2020).

- Our results provide new support for the hypothesis of a tectonically active Moon (e.g., Watters et al., 2010; Banks et al., 2012; Watters et al., 2010; Clark et al., 2017; Van der Bogert et al., 2018; Watters et al., 2019; Williams et al., 2019; Lu et al., 2019; Valantinas and Schultz, 2020). The addition of recently active mare wrinkle ridges to prior observations of recently active lobate scarps in the lunar highlands provides a more complete the global understanding recent lunar tectonism. As such, the lunar mare should be considered as a target of interest for future lunar seismic analysis missions.

Acknowledgements

The authors would like to acknowledge productive discussions with Caleb Fassett, Peter Schultz, Adomas Valantinas, Jaclyn Clark, and members of the Mini-RF instrument science team that improved this effort. This work was supported in part by NASA Lunar Data Analysis Program (LDAP) NNX17AI80G and a grant from the Johns Hopkins University Applied Physics Laboratory through the NASA LRO mission.

Data availability statement

The recently active wrinkle ridge and crosscut impact crater datasets generated in this work and presented in figure 2 are available in a Figshare repository (https://figshare.com/s/a2c308f4df7e9bf336cc) as GIS-ingestible shapefiles in an Equirectangular coordinate system. The image data used to map and create those datasets are publicly available through the LROC QuickMap web interface (https://quickmap.lroc.asu.edu).

References

Andrews-Hanna, J. C., Besserer, J., Head III, J. W., et al., (2014). Structure and evolution of the lunar Procellarum region as revealed by GRAIL gravity data. Nature, 514(7520), 68-71.

Banks, M. E., Watters, T. R., Robinson, M. S., Tornabene, L. L., Tran, T., Ojha, L., & Williams, N. R. (2012). Morphometric analysis of small-scale lobate scarps on the Moon using data from the Lunar Reconnaissance Orbiter. Journal of Geophysical Research: Planets, 117(E12). https://doi.org/10.1029/2011JE003907

Binder, A. B. (1982). Post-Imbrian global lunar tectonism: Evidence for an initially totally molten Moon. The moon and the planets, 26(2), 117-133.

Clark, J. D., Bernhardt, H., Robinson, M. S., (2022). Extensional features at east Serenitatus wrinkle ridge-lobate scarp transition indicate recent tectonic activity. In 52nd Annual Lunar and Planetary Science Conference (No. 1305).

Clark, J. D., Hurtado, J. M., Hiesinger, H., van der Bogert, C. H., & Bernhardt, H. (2017). Investigation of newly discovered lobate scarps: Implications for the tectonic and thermal evolution of the Moon. Icarus (New York, N.Y. 1962), 298, 78–88. https://doi.org/10.1016/j.icarus.2017.08.017

Fassett, C. I., & Thomson, B. J. (2014). Crater degradation on the lunar maria: Topographic diffusion and the rate of erosion on the Moon. Journal of Geophysical Research: Planets, 119(10), 2255-2271.

Freed, A. M., Melosh, H. J., & Solomon, S. C. (2001). Tectonics of mascon loading: Resolution of the strike-slip faulting paradox. Journal of Geophysical Research: Planets, 106(E9), 20603–20620. https://doi.org/10.1029/2000JE001347

Hiesinger, H., Head, J. W., Wolf, U., Jaumann, R., & Neukum, G. (2011). Ages and stratigraphy of lunar mare basalts: A synthesis. Recent advances and current research issues in lunar stratigraphy, 477, 1-51.

Lu, Y., Wu, Y., Michael, G. G., Basilevsky, A. T., & Li, C. (2019). Young wrinkle ridges in Mare Imbrium: Evidence for very recent compressional tectonism. Icarus (New York, N.Y. 1962), 329, 24–33. https://doi.org/10.1016/j.icarus.2019.03.029

Melosh, H. J. (1978). The tectonics of mascon loading. In Lunar and planetary science conference proceedings (Vol. 9, pp. 3513-3525).

Melosh, H. J. (1980). Tectonic patterns on a tidally distorted planet. Icarus, 43(3), 334-337.

Moore, H. J., Boyce, J. M., & Hahn, D. A. (1980). Small impact craters in the lunar regolith—Their morphologies, relative ages, and rates of formation. The moon and the planets, 23(2), 231-252.

Schleicher, L. S., Watters, T. R., Martin, A. J., & Banks, M. E. (2019). Wrinkle ridges on Mercury and the Moon within and outside of Mascons. Icarus, 331, 226-237.

Schultz, P. H. (1976). Moon morphology: Interpretations based on Lunar Orbiter photography. Austin: University of Texas Press.

Schultz, P. H., & Crawford, D. A. (2011). Origin of nearside structural and geochemical anomalies on the Moon. Geological Society of America Special Papers, 477, 141-159.

Schultz, P. H., & Spudis, P. D. (1983, March). The beginning and end of mare volcanism on the Moon. In Lunar and Planetary Science Conference (Vol. 14, pp. 676-677).

Solomon, S. C., & Head, J. W. (1980). Lunar Mascon Basins: Lava filling, tectonics, and evolution of the lithosphere. Reviews of Geophysics (1985), 18(1), 107–141. https://doi.org/10.1029/RG018i001p00107

Speyerer, E. J., Povilaitis, R. Z., Robinson, M. S., Thomas, P. C., & Wagner, R. V. (2016). Quantifying crater production and regolith overturn on the Moon with temporal imaging. Nature, 538(7624), 215-218.

Thompson, T.J., Robinson, M.S., Watters, T.R. and Johnson, M.B., (2017). March. Global lunar wrinkle ridge identification and analysis. In 48th Annual Lunar and Planetary Science Conference (No. 2665).

Tian, H. C., Wang, H., Chen, Y., et al., (2021). Non-KREEP origin for Chang'e-5 basalts in the Procellarum KREEP Terrane. Nature, 600(7887), 59-63.

Trask, N. J. (1971). Geologic comparison of mare materials in the lunar equatorial belt, including Apollo 11 and Apollo 12 landing sites. US Geol. Surv. Prof. Pap., 750D, 138-148.

Valantinas, A., & Schultz, P. H. (2020). The origin of neotectonics on the lunar nearside. Geology (Boulder), 48(7), 649–653. https://doi.org/10.1130/G47202.1

van der Bogert, C. H., Clark, J. D., Hiesinger, H., Banks, M. E., Watters, T. R., & Robinson, M. S. (2018). How old are lunar lobate scarps? 1. Seismic resetting of crater size-frequency distributions. Icarus (New York, N.Y. 1962), 306, 225–242. https://doi.org/10.1016/j.icarus.2018.01.019

Watters, T. R. (2022). Lunar Wrinkle Ridges and the Evolution of the Nearside Lithosphere. Journal of Geophysical Research: Planets, e2021JE007058.

Watters, T. R., Robinson, M. S., Banks, M. E., Tran, T., & Denevi, B. W. (2012). Recent extensional tectonics on the Moon revealed by the Lunar Reconnaissance Orbiter Camera. Nature Geoscience, 5(3), 181–185. https://doi.org/10.1038/ngeo1387

Watters, T. R., Weber, R. C., Collins, G. C., Howley, I. J., Schmerr, N. C., & Johnson, C. L. (2019). Shallow seismic activity and young thrust faults on the Moon. Nature Geoscience, 12(6), 411–417. https://doi.org/10.1038/s41561-019-0362-2

Watters, T.R., Robinson, M. S., Beyer, R. A., Banks, M. E., Bell, 3rd, Pritchard, M. E., Hiesinger, H., van der Bogert, C. H., Thomas, P. C., Turtle, E. P., & Williams, N. R. (2010). Evidence of Recent Thrust Faulting on the Moon Revealed by the Lunar Reconnaissance Orbiter Camera. Science (American Association for the Advancement of Science), 329(5994), 936–940. https://doi.org/10.1126/science.1189590

Watters, T.R., Robinson, M. S., Collins, G. C., Banks, M. E., Daud, K., Williams, N. R., & Selvans, M. M. (2015). Global thrust faulting on the Moon and the influence of tidal stresses. Geology (Boulder), 43(10), 851–854. https://doi.org/10.1130/G37120.1

Williams, N. R., Bell III, J. F., Watters, T. R., Banks, M. E., Daud, K., & French, R. A. (2019). Evidence for recent and ancient faulting at Mare Frigoris and implications for lunar tectonic evolution. Icarus (New York, N.Y. 1962), 326, 151–161. https://doi.org/10.1016/j.icarus.2019.03.002

Yue, Z., Li, W., Di, K., Liu, Z., & Liu, J. (2015). Global mapping and analysis of lunar wrinkle ridges: LUNAR WRINKLE RIDGES GLOBAL MAPPING. Journal of Geophysical Research. Planets, 120(5), 978–994. https://doi.org/10.1002/2014JE004777

Yue, Z., Michael, G., Di, K., & Liu, J. (2017). Global survey of lunar wrinkle ridge formation times. Earth and Planetary Science Letters, 477, 14–20. https://doi.org/10.1016/j.epsl.2017.07.048